ACS APPLIED MATERIALS & INTERFACES

www.acsami.org

Research Article

Suppression of Membrane Degradation Accompanied with Increased Output Performance in Fuel Cells by Use of Silica-Containing Anode Catalyst Layers

Mohamed R. Berber, Muhammad Imran, Hanako Nishino, and Hiroyuki Uchida*

Cite This: *ACS Appl. Mater. Interfaces* 2023, 15, 13219–13227

Read Online

ACCESS | Metrics & More | Article Recommendations | Supporting Information

ABSTRACT: Polymer electrolyte membranes (PEMs) for fuel cells are chemically degraded by the attack of ·OH radicals generated from the decomposition of H_2O_2, which is predominantly produced at the Pt/C hydrogen anode. The incorporation of conventional radical scavengers into the PEM suffers from a decrease in the output performance. We, for the first time, demonstrate that the addition of hygroscopic silica nanoparticles (NPs) to the Pt/C anode catalyst layer provides a remarkably prolonged (ca. 4 times) lifetime of a Nafion membrane in an accelerated stress test and open circuit voltage (OCV) holding at 90 °C, accompanied by improved output (I–E) performances at low relative humidity. It has been found that the use of silica NPs decreases H_2O_2 formation rate from the OCV to a practical H_2 oxidation potential in a half-cell using 0.1 M $HClO_4$ at 90 °C and provides reduced ohmic resistance (increase in water content) and effective utilization of Pt cathode catalyst in a single cell, by which the improvement of the durability of the PEM and increased output performance are explained rationally.

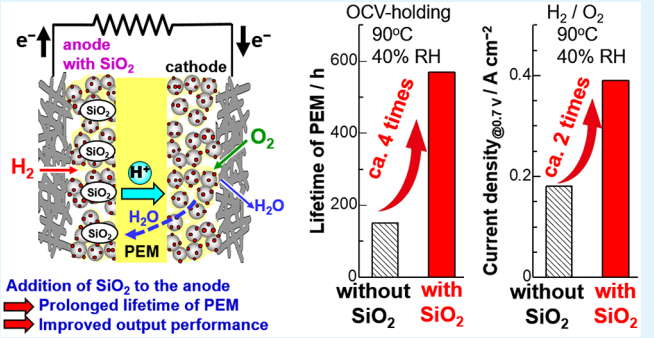

KEYWORDS: *polymer electrolyte fuel cell, anode catalyst layer, silica, perfluorinated sulfonic acid membrane, durability*

1. INTRODUCTION

The membrane electrode assembly (MEA) is the core component of polymer electrolyte fuel cell (PEFC) technology that is projected for applications in fuel cell vehicles (FCVs) and residential cogeneration systems. A typical MEA comprises a polymer electrolyte membrane (PEM) and two Pt-based catalyst layers (CLs), which are coated on a PEM to catalyze the hydrogen oxidation reaction (HOR) and oxygen reduction reaction (ORR). Despite extensive efforts to improve the performance and durability while reducing the cost for widespread commercialization, the MEA components still face a number of issues.[1−4]

The PEM plays an essential role in the proton conduction in the MEA as well as a separation of fuel gas (H_2) and oxidant (air).[4] Perfulorinated sulfonic acid (PFSA) polymers such as Nafion have been employed as the PEM due to their high proton conductivity (σ_H) and chemical stability with acceptable properties for gas permeability and mechanical strength. Recently, very thin PEMs have been used to enhance the cell performance via low ohmic resistance and high back-diffusion rate of water.[4,5] However, the increased permeation rates of H_2 and O_2 through the thinner PEMs induce penalties of decreased cathode potential, decreased fuel efficiency, and decreased membrane durability due to chemical degradation. The increase in permeation rate of O_2 through the PEM from the cathode results in the increased production rate of H_2O_2 at Pt particles supported on carbon (Pt/C) anode for the HOR.[4,6] Hydroxyl radicals (·OH) generated via the reaction of H_2O_2 with impurities (such as Fe^{2+}) can lead to severe degradation of the PEM, including thinning of the membrane and, subsequently, perforation damage.[4,6,7] Therefore, the suppression of the chemical degradation of the PEM is an issue of high concern that urgently requires a solution.

The incorporation of radical scavengers/quenchers (i.e., CeO_2, TiO_2, ZrO_2, MnO_2, and other metal oxides) into the PEM or CLs has been effective in mitigating the decomposition rate of the PEM.[7−11] However, a serious drawback has been recognized in the use of radical scavengers based on redox reactions of transition-metal cations; i.e., the ion exchange of the metal cations such as Ce^{3+} lowered the σ_H of the electrolyte, both the membrane itself and the ionomer in the cathode CL, resulting in severe polarization loss.[12,13] Thus,

Received: January 31, 2023
Accepted: February 21, 2023
Published: February 28, 2023

it is of the utmost importance to escape the trade-off between the PEM durability and output performance that exists for the radical scavengers employed so far.

Here, we propose a unique concept with the use of hygroscopic silica nanoparticles (NPs). Distinct from the transition-metal oxides stated above, silica (typical-metal oxide) is neither oxidized by ·OH radicals nor reduced by H_2. It has been reported that the incorporation of SiO_2−NPs in a Nafion membrane increased the σ_H, specifically at low relative humidity (RH), due to its hygroscopic property.[14,15] Recently, Inoue et al. added silica NPs to the anode and cathode CLs of gas diffusion electrodes (GDE) to increase the effective utilization of Pt catalysts under low RH conditions,[16,17] while Park et al. reported an increase in the cell performance by coating an SiO_2 layer on Pt/C cathode catalysts.[18] On the basis of these results, it is envisioned that the addition of hygroscopic silica NPs leads to a longer residence time of H_2O_2 molecules within the anode CL, leading to a longer lifetime of the Nafion membrane, as well as an increase in the effective utilization of the Pt catalyst.

In the present work, the durability of MEAs with silica-containing anode CLs has been examined by use of an accelerated stress test (AST) as a function of silica content. Remarkable changes in the steady-state polarization curves (I−E curves) and ohmic resistances at low RH are also shown.

2. EXPERIMENTAL SECTION

2.1. Materials. The Nafion membrane (NRE-211; 25 μm in thickness, denoted as Nafion-PEM), commercial Pt/carbon black catalyst (denoted as Pt/C) for the anode (TEC10E50E, 46.4 wt % of Pt, d_{Pt} = 2.4 ± 0.5 nm, Tanaka Kikinzoku Kogyo K.K., Japan), heat-treated Pt/graphitized carbon black catalyst (denoted as Pt/GCB-HT) for the cathode (TEC10EA50E-HT, 50.2 wt % of Pt, d_{Pt} = 7.4 ± 1.4 nm, Tanaka Kikinzoku Kogyo K. K., Japan), Nafion binder solution (IEC = 0.95−1.03 mequiv g^{-1}; 20% dispersion, DE-521, E. I. Du Pont de Nemours & Co. Inc.), tetraethyl orthosilicate (TEOS) as a source of silica, ethanol (purity 99.5%), 1 M HNO_3 solution, and 0.1 M $HClO_4$ solution. The Pt/GCB-HT cathode catalyst was chosen to minimize any change in the performance during a long-term AST, while the Pt/C anode catalyst is a typical one that is widely used.

2.2. Preparation of MEAs. Catalyst-coated membranes (CCMs) were fabricated in a similar manner to that described in the literature.[19] Details of the procedure are explained in Section S1 of the Supporting Information. Briefly, the CCM comprised a Pt/C anode CL (with and without SiO_2), Nafion-PEM, and Pt/GCB-HT CL. A silica colloidal solution was prepared by the hydrolysis and condensation of a TEOS solution by adding 1.0 M HNO_3.[16,17] A given amount of silica colloidal solution was added to the anode catalyst paste. While the general formula of silica NPs in the colloidal solution can be written as $SiO_x(OH)_{4-2x}$ (x < 2),[20] we assume a formula of SiO_2 for convenience to describe the composition of anode CLs. A volume ratio of SiO_2 to carbon in the Pt/C catalyst (V_{SiO_2}/V_C) was employed as the representative parameter, which ranged from 0.1 to 0.4. The reason for the use of V_C is that the volume of carbon (density = 2.25 g cm^{-3}) is predominant in the CL, i.e., 11 times larger than that of Pt (21.37 g cm^{-3}, 46.4 wt % in Pt/C). The mass ratio of Nafion binder to the carbon support (N/C ratio), which is nearly equal to the volume ratio, in all CLs was controlled to 0.70 (dry basis). The geometric area and Pt loading amount in all CLs were 29.2 cm^2 and 0.50 ± 0.01 mg cm^{-2}, respectively. The reason for such a high Pt loading anode was to accelerate the H_2O_2 formation rate.[21] A high Pt loading at the cathode was used to maintain a sufficient active area for the Pt/GCB-HT catalyst with a relatively low electrochemically active surface area (ECSA). Each CCM with two gas diffusion layers (GDLs, 22BB, SGL Carbon Group) was mounted into a Japan Automobile Research Institute (JARI) cell. The contents of SiO_2 in the anode CL are denoted as 0.1-SiO_2, 0.2-SiO_2, 0.3-SiO_2, and 0.4-SiO_2 for the volume ratios V_{SiO_2}/V_C of 0.1, 0.2, 0.3, and 0.4, respectively. The values of the volume ratio and mass ratio for SiO_2/C and SiO_2/Pt in these anode CLs are summarized in Table S1.

The morphology and elemental distribution of Pt, Si, C, F, and S for the anode CL in the pristine state were observed by a scanning transmission electron microscope (STEM, Hitachi High Technologies, Co., HD-2700, acceleration voltage = 200 kV) equipped with an energy-dispersive X-ray spectrometer (EDX, Bruker Corp., X Flash 5030).

2.3. Test Protocols for Single Cells. Before the tests, the single cell was conditioned by repeating stepwise increase/decrease of current density at the cell temperature T_{cell} of 40 °C with fully humidified H_2 and O_2 (100% RH) at a constant flow rate of 100 mL min^{-1} for both gases. Then, the T_{cell} was elevated to 90 °C, at which all measurements were performed.

At the beginning of testing (BOT), every 200 h of the AST, and at the end-of-life (EOL), the values of hydrogen-leak current density $j(H_2)$ at the cathode and ECSA for the anode and cathode were measured by use of linear sweep voltammetry (LSV) and cyclic voltammetry (CV), respectively, at 40% RH, 90 °C, and ambient pressure.[19] The steady-state polarization curves (I−E curves) at T_{cell} = 90 °C and ambient pressure were also measured galvanostatically at the BOT. Hydrogen gas humidified at 20% or 40% RH was supplied to the anode with a utilization of 70%, and oxygen gas humidified at 40% or 60% RH was supplied to the cathode with a utilization of 40%. The ohmic resistances were measured at 1 kHz by use of a digital AC milliohm meter (Tsuruga Denki, Model 3566).[19]

The chemical stability of the MEAs was examined via an AST in which the single cell was maintained at OCV in H_2/air at T_{cell} = 90 °C with 40% RH and a back-pressure of 160 kPa-G. The flow rates of H_2 and air were maintained at 200 mL min^{-1}. The conditions of the present AST (90 °C, 40% RH, and 160 kPa-G) are somewhat different from those recommended by the U.S. DRIVE Fuel Cell Tech Team (90 °C, 30% RH, and 150 kPa_{abs}).[22] The relative humidity of 40% RH was chosen because the degradation rate of Nafion membranes at 40% RH was reported to be comparable to that at 30% RH (nearly constant from 30% to 40% RH) at 90 to 100 °C,[23,24] and we found that the I−E curves measured at 40% RH reached a steady state much more quickly than was the case at 30% RH. With regard to the gas pressures, a higher partial pressure of O_2 accelerated the degradation rate,[23] and 160 kPa-G has been employed in our previous work in collaboration with a Japanese car company.[19]

The AST was continued until the OCV decreased to 0.85 V (ca. 10% loss of the initial OCV). The effluent water from both electrodes was collected every 50 h to analyze fluoride ions emitted from the MEA by use of an ion chromatography instrument at the Yamanashi Research Center for Environmental Science. The microstructure and elemental distribution of Pt, Si, and F for the cross section of MEA before and after the AST were observed by a scanning electron microscope (SEM, Hitachi High-Technologies Co., SU3500) with an EDX (Oxford Instruments, Xplore 30).

2.4. Measurement Methods of H_2O_2 Formation Rates and HOR Activities on Catalysts in 0.1 M $HClO_4$ Solution (Half-Cell). By a similar protocol as that previously reported in the literature,[21,25] HOR activities and H_2O_2 formation rates on (Pt/C + silica) were measured with hydrodynamic voltammetry in 0.1 M $HClO_4$ solution using the multichannel flow double electrode (m-CFDE) technique at 80 and 90 °C. The electrolyte solution used was 0.1 M $HClO_4$, which was purified in advance by pre-electrolysis methods.[26] The working electrode (WE) was Pt/C + silica with Nafion binder (the identical ink used in the anode CL in CCM) dispersed on an Au substrate at 12 μg_{Pt} cm^{-2}. The electrode potential was referred to the reversible hydrogen electrode RHE(t) (t = 80 or 90 °C). The kinetically controlled specific activity j_k and mass activity MA_k for the HOR of 4 WEs were evaluated simultaneously in H_2-saturated solution at a sweep rate of 1 mV s^{-1}. The H_2O_2 emitted from each WE, $j(H_2O_2)$, in O_2-saturated solution was detected at a Pt-collecting electrode (located downstream of each WE) whose

https://doi.org/10.1021/acsami.3c01392
ACS Appl. Mater. Interfaces 2023, 15, 13219−13227

potential was held at 1.4 V. Details of the m-CFDE technique are described in Section S2 of the Supporting Information.

3. RESULTS AND DISCUSSION

3.1. Effect of Silica in the Anode CL on Degradation of Nafion Membrane during the OCV Test of Single Cells. Figure 1 shows the time course of the OCV, H_2-leak current density $j(H_2)$, and the total amount of fluoride (F^-) ions emitted during the AST at T_{cell} = 90 °C by maintaining the OCV of single cells with the anode CLs containing various silica volume ratios. The initial values of ECSA for the anode CLs were nearly independent of the silica volume ratios (62.4 ± 4.0 $m^2\ g_{Pt}^{-1}$), and those for the cathode CLs were approximately identical (23.9 ± 4.0 $m^2\ g_{Pt}^{-1}$) in all cells. As a measure of the durability of the membrane, the lifetime is defined as the time at which the OCV reached 0.85 V; this has been plotted as a function of V_{SiO_2}/V_C in Figure S1. It has been reported for the chemical degradation of the Nafion membrane by ·OH radical attack that F^- ions are emitted, which accompanies the decrease in the thickness of the membrane[7] (or pinhole formation[19]), by which $j(H_2)$ increases and OCV decreases. The OCV of the cell without silica in the anode rapidly dropped after ca. 80 h and reached values below 0.85 V at 150 h with a high $j(H_2)$ (36 times higher than the initial value) and high fluoride emission rate (FER, slope of the line in Figure 1c) detected in the effluent water. With the addition of silica in the anode CL, the lifetime increased remarkably, and it nearly leveled off (550−620 h) for $V_{SiO_2}/V_C \geq 0.2$.

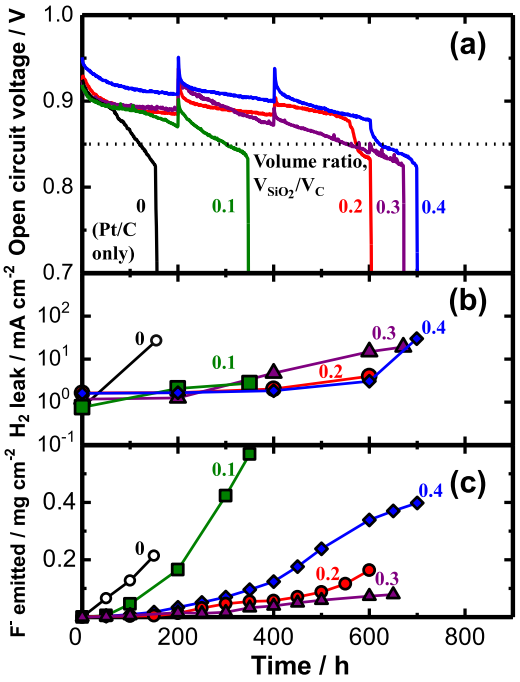

Figure 1. Changes in (a) open circuit voltage (OCV), (b) H_2-leak current density, and (c) total amount of F^- ions emitted (from anode and cathode) with time in the AST of single cells with various anode CLs at T_{cell} = 90 °C, 40% RH (H_2/air), and 160 kPa-G.

The value of $j(H_2)$ was evaluated as the limiting current density (j_L) in the LSV for the oxidation of H_2 crossing over from the H_2 anode to the cathode compartment in a N_2 atmosphere (Figure 1b). Changes in the LSVs for each cell with various anode CLs are shown in Figure S2. Except for LSVs taken close to the EOL, a distinct j_L value independent of the potential was observed from ca. 0.2 to 0.6 V. However, after the degradation of the Nafion PEMs (typically shown in Figure S2, at 155 h in (a), 600 and 671 h in (d), and 699 h in (e)), the slopes of the voltammograms increased, which can most likely be ascribed to an electronic conductance (micro-short circuit) through the Nafion PEM superposed onto the j_L for the HOR. Hence, the current density at 0.4 V in the voltammogram was taken as the $j(H_2)$, which is one of the important parameters indicating the degree of degradation. The increases in $j(H_2)$ were found to be much smaller for the cells with silica than that for the cell without silica.

An appreciable mitigation of the degradation of the Nafion PEM resulting from the presence of silica was clearly seen for changes in the emission of F^- with time in Figure 1c. For $V_{SiO_2}/V_C \geq 0.2$, the emission of F^- was suppressed at very low levels during the initial 150 h. The value of FER was at a minimum for 0.2-SiO_2 and 0.3-SiO_2 and increased again at 0.4-SiO_2. The lowest FER at 0.3-SiO_2 was 1 order of magnitude less than that without silica. The total amount of F^- of 0.1 mg cm^{-2} emitted from the cell with 0.3-SiO_2 (after 600 h) corresponds to about 3% loss of F content in the Nafion PEM[27] with 25 μm thickness. Thus, a noticeably prolonged lifetime of the Nafion PEM has been demonstrated for the anode CL containing silica NPs by the single cell test. An inconsistency between the lowest FER and a relatively large $j(H_2)$ for 0.3-SiO_2 could be due to some artifact in the LSV measurement seen in Figure S2d.

It is very important to clarify how silica NPs were dispersed in the anode CL and whether silica NPs remained stable in the CL or not. First, the microstructure and elemental distribution of Pt, Si, C, F, and S for 0.2-SiO_2 anode CL in the pristine state were observed by a STEM with EDX. As shown in Figure 2, the elemental distribution of Si was found to be very uniform in the CL. The amount of Si was quantitatively analyzed for the EDX spectrum, resulting in the mass ratio m_{Si}/m_{Pt} of 0.12, which exactly coincides with that loaded for the 0.2-SiO_2 anode CL (see Table S1). The high-resolution images (TEM bright-field images) of the same sample are shown in Figure S3. It was difficult to identify silica NPs clearly, but faint images of NPs of less than 5 nm were seen (dotted circles, for example), which can be distinguished from the Nafion binder and carbon support. One of the possible reasons for such faint images in TEM is the low electron absorption cross section of SiO_2. Another reason is with certainty their low crystallinity, i.e., with remaining OH groups. Indeed, a broad peak at 2θ = 22.5° assigned to the amorphous phase of SiO_2 was observed at in X-ray diffraction (XRD) of silica even after drying the colloidal solution (Figure S4).

Figure 3 shows SEM images and the elemental distribution of Si, Pt, and F (line analysis, measured by EDX) in the cross section of the MEA with a 0.2-SiO_2 anode CL in the pristine state and after the AST for 600 h. It was found that the Si component remained at the anode CL; i.e., the boundary of the Si coincided well with that of Pt in the CL even after 600 h. Considering the decomposition ratio (at most 5%) of the Nafion PEM stated above, a reduction of the membrane thickness by ca. 10% in the SEM image can be ascribed to that due to the fastening pressure in the cell.

3.2. H_2O_2 Formation Rate and HOR Activities at Pt/C with Addition of Silica. To examine the mechanism of the prolonged lifetime of the membranes by silica NPs added in

https://doi.org/10.1021/acsami.3c01392
ACS Appl. Mater. Interfaces 2023, 15, 13219−13227

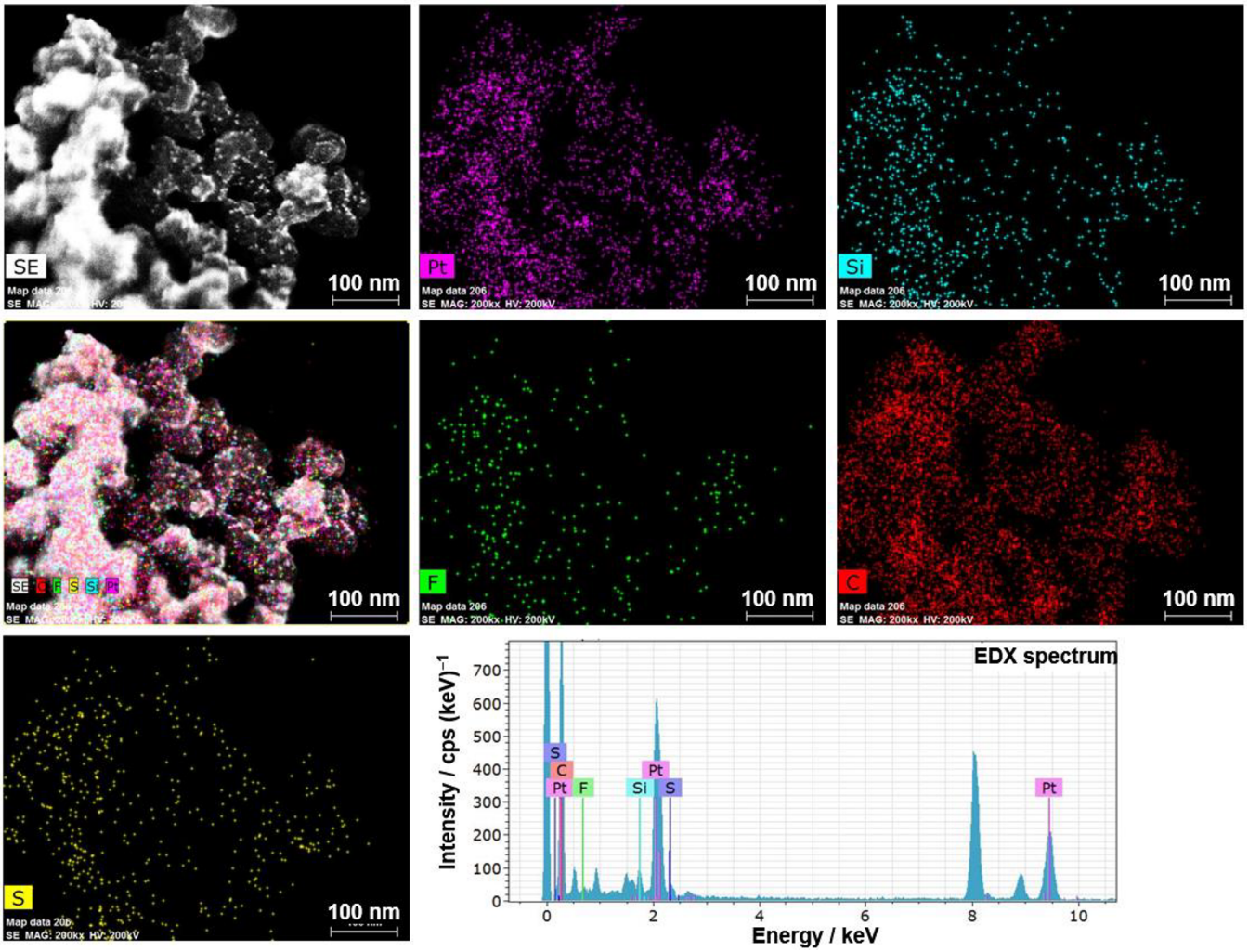

Figure 2. Microstructure [secondary electron (SE) image], elemental distribution of Pt, Si, C, F, and S, and energy-dispersive X-ray spectrum for the 0.2-SiO_2 anode CL in the pristine state. A droplet of the anode paste was dried on a microgrid for the observation.

the anode CL, the H_2O_2 formation rate and HOR activities were measured in 0.1 M $HClO_4$ solution by the m-CFDE technique at 80 and 90 °C. Figure 4 shows the potential dependence of $j(H_2O_2)$ on Pt/C without and with various silica content at 90 °C. The values of $j(H_2O_2)$ for all samples were highest at 0 V vs RHE (corresponding to the open circuit condition in the single cell) and decreased with increasing potential, consistent with the tendency in our previous work measured at 80 °C.[21,25] With the addition of silica, the values of $j(H_2O_2)$ decreased remarkably. As shown in Figure 5, $j(H_2O_2)$ values at 0 V exhibited the minimum value at V_{SiO_2}/V_C of 0.1 and 0.2, which was less than 1/3 of that measured without silica. In contrast, the HOR activities (both MA_k and j_k) were nearly unchanged irrespective of V_{SiO_2}/V_C from 0 to 0.4. Similar tendencies were observed at 80 °C, as shown in Figures S5 and S6. Thus, the addition of silica NPs in the Pt/C anode markedly suppressed the formation of H_2O_2, which contributed to the enhancement in the lifetime of the Nafion PEMs in the single cells, without affecting the HOR activity.

Recently, in our group, $j(H_2O_2)$ at a Pt-skin-covered PtCo/C catalyst was found to be suppressed as much as 50%, together with enhanced HOR activity, compared with Pt/C, which was ascribed to the lowered binding energy of hydrogen atoms adsorbed on the Pt skin with modified electronic structure, as modeled with DFT calculations.[25] The weakened H adsorption with narrowing of the d band at Pt skin/PtCo was also confirmed by in situ X-ray absorption near-edge structure (XANES).[28] It is essential to understand how the silica NPs worked as a promoter in suppressing H_2O_2 formation at Pt/C without changing the HOR activity. It has been reported that SiO_2 (silica gel) forms a complex with H_2O_2 due to their strong interaction.[29] Such a "trapped" H_2O_2 could be decomposed to H_2O by the Pt/C catalyst in the working electrode of the m-CFDE as well as the anode CL of a single cell. However, it is noteworthy that the dependence of $j(H_2O_2)$ on V_{SiO_2}/V_C in 0.1 M $HClO_4$ (Figure 5) was different from the behavior that the degradation rate in the AST of a single cell reached a minimum at a V_{SiO_2}/V_C of 0.2 and 0.3 with respect to the FER (Figure 1c). One of the possible reasons for the difference is proposed to be the humidity level (solution phase in the m-CFDE vs 40% RH in the single cell); we are therefore considering the ways in which the hydration of the SiO_2 affects its interaction with H_2O_2, as discussed later, as well as a possible additional mechanism for the mitigation of degradation.

3.3. *I*–*E* Performance and Ohmic Resistance of Single Cells at Various RH Levels. To evaluate the effect of silica loading in the anode CL on the cell performances, single cells

https://doi.org/10.1021/acsami.3c01392
ACS Appl. Mater. Interfaces 2023, 15, 13219−13227

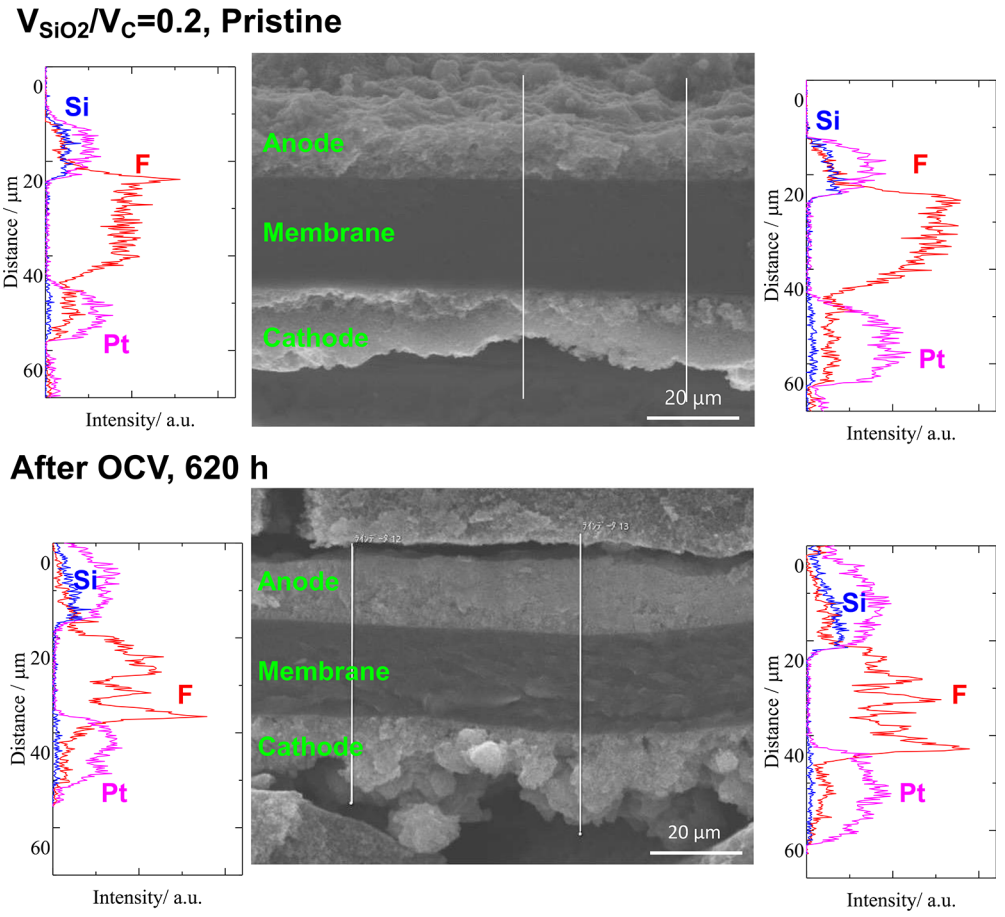

Figure 3. SEM images and elemental distribution of Si, F, and Pt (measured by EDX) in the cross section of MEA with 0.2-SiO_2 anode CL in the pristine state and after the AST for 600 h.

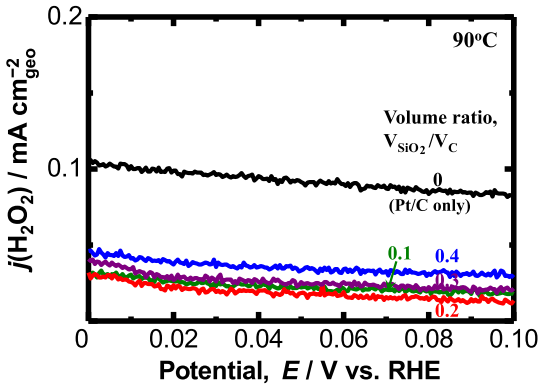

Figure 4. H_2O_2 formation current density $j(H_2O_2)$ on Pt/C with various silica volume ratios at 90 °C for the potential range from 0 to 0.1 V vs RHE in O_2-saturated 0.1 M $HClO_4$ solution with a mean flow rate of 17.5 cm s^{-1} and Pt loading of 12 μg_{Pt} cm^{-2}.

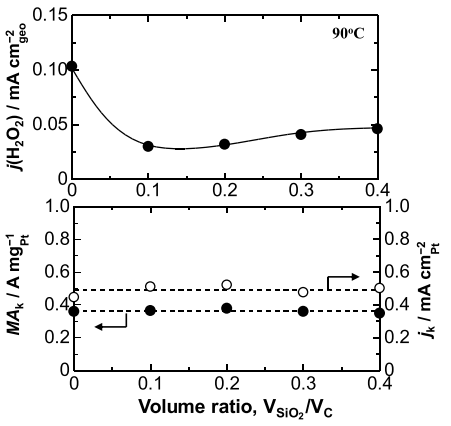

Figure 5. Dependences of H_2O_2 formation current density $j(H_2O_2)$ (at 0 V vs RHE in O_2-saturated 0.1 M $HClO_4$), kinetically controlled mass activity MA_k and specific current density j_k for the HOR (at 0.02 V vs RHE in H_2-saturated solution) on volume ratio of V_{SiO_2}/V_C at 90 °C with 12 μg_{Pt} cm^{-2}.

were operated by supplying H_2 and O_2 at T_{cell} = 90 °C with different RH levels under ambient pressure. In addition to uniform humidity at 40% RH for both gases, asymmetric RH levels, 20% RH H_2/40% RH O_2, and 20% RH H_2/60% RH O_2 were examined, considering that in FCVs dry H_2 from a pressurized tank is supplied to the anode, followed by humidification with water back-diffusing from the cathode. Figure 6 shows the steady-state polarization curves (I–E curves) and ohmic resistances (R_{ohm}) for cells operated with 20% RH H_2/40% RH O_2. Similar data taken at other RH levels are shown in Figures S7 and S8. The addition of silica NPs in the anode CL gave rise to higher I–E performance and lower R_{ohm} values over the whole current density range examined. Thus, we have for the first time, demonstrated an excellent role of silica NPs in improving the durability of PEMs accompanied by increased output performance of single cells, which is distinct from the trade-off effect of conventional radical

https://doi.org/10.1021/acsami.3c01392
ACS Appl. Mater. Interfaces 2023, 15, 13219−13227

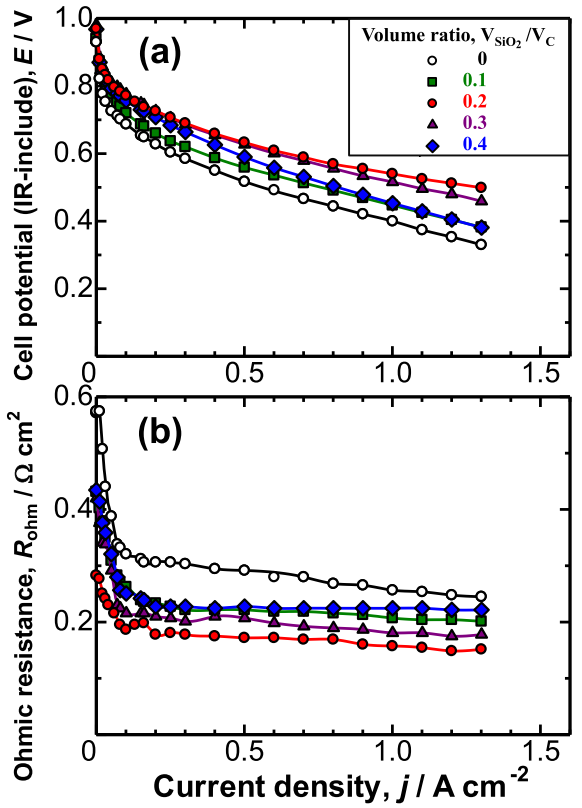

Figure 6. Steady-state polarization (I–E) curves (a) and ohmic resistances R_{ohm} (b) of single cells with various anode CLs operated at T_{cell} = 90 °C with 20% RH H_2/40% RH O_2 under ambient pressure. The utilizations of H_2 and O_2 were 70% and 40%, respectively.

scavengers. Next, we discuss the role of the silica NPs in the anode CL.

The values of R_{ohm} measured at 0.40 A cm^{-2} under various RH levels are plotted as a function of V_{SiO_2}/V_C in Figure 7. The values of R_{ohm} decreased with increasing RH and were nearly at the same level at 40% RH//40% RH and 20% RH//60% RH within the measurement error of the AC milliohm meter. For

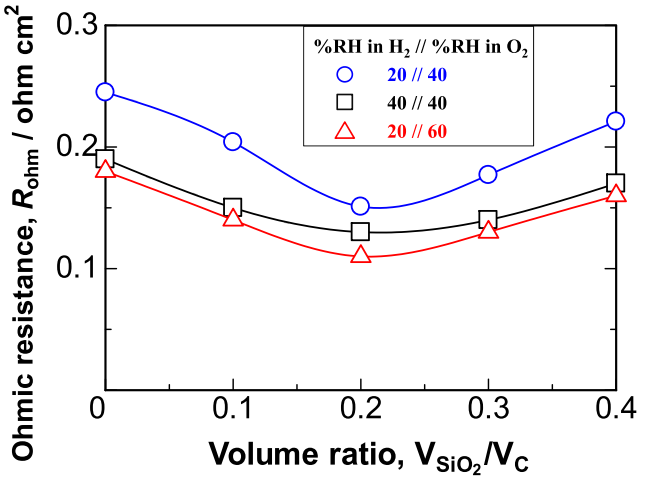

Figure 7. Plots of ohmic resistances R_{ohm} (measured at 0.4 A cm^{-2}) in the single cells as a function of V_{SiO_2}/V_C in the anode CLs under three different RH levels at 90 °C and ambient pressure. The utilizations of H_2 and O_2 are identical with those in Figure 6.

all RH levels, R_{ohm} exhibited a minimum at V_{SiO_2}/V_C from 0.2 to 0.3. Such a decrease in R_{ohm} clearly corresponds to the increase in the proton conductance of Nafion in the PEM and binder in the CLs due to an increased hydration level (water content), which is consistent with our previous work:[16,17] hygroscopic silica NPs maintained a high water content in Nafion via promoting the back-diffusion of water from the cathode.

The reduction of R_{ohm}, of course, decreases the ohmic (IR) loss, i.e., increasing the cell potential. For example, under 20% RH//40% RH, the R_{ohm} value at 0.2-SiO_2 decreased by 0.094 ohm cm^2, compared with that without silica, providing a voltage gain of 0.038 V at 0.40 A cm^{-2}. In contrast, the cell potential at 0.2-SiO_2 and the identical current density was higher by 0.109 V than that without silica, suggesting that the decrease in R_{ohm} was not predominant in the improvement of the I–E performance. Then, the mass activities (MA) at 0.85 V and current densities at 0.70 V ($j_{@0.7V}$) are plotted as a function of V_{SiO_2}/V_C in Figure 8. The former is a measure of the

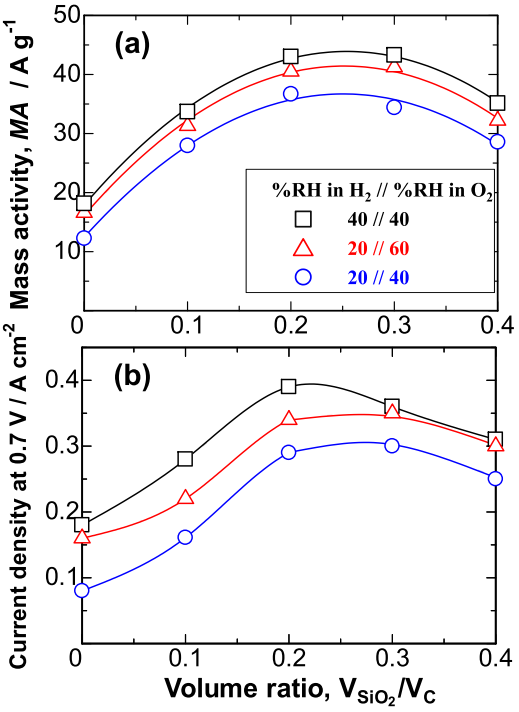

Figure 8. Effect of silica volume ratio (V_{SiO_2}/V_C in the anode CL) on mass activity at 0.85 V (a) and current density at 0.7 V (b) under three RH levels at 90 °C. The utilizations of H_2 and O_2 are identical with those in Figure 6.

effectiveness of Pt in the cathode CL with little influence of mass transport[30] because the overpotential at the Pt/C anode with pure H_2 was negligibly small at a Pt loading of 0.5 mg_{Pt} cm^{-2} even at low RH,[31] and the kinetically controlled HOR activities were not affected by silica, as stated above. On the other hand, the latter reflects the overall factors of effectiveness of Pt, proton conductance in the CL, and gas transport (O_2 and H_2O).[31] Both MA and $j_{@0.7V}$ reached a plateau at V_{SiO_2}/V_C between 0.2 and 0.3, as in the case of R_{ohm}. It was also found that the enhancement factor for MA or $j_{@0.7V}$ by silica addition was larger at low RH. The value of MA at 0.2-SiO_2 was higher than that without silica by a factor of 3 under 20% RH//40%

https://doi.org/10.1021/acsami.3c01392
ACS Appl. Mater. Interfaces 2023, 15, 13219−13227

RH, while the factor decreased to 1.9 under 40% RH//40% RH. Thus, the major factor for the improvement of *I*–*E* performance by silica is with certainty, ascribed to the increase in water content of Nafion in the cathode CL.

Even under OCV conditions, a small amount of water (a few mA cm^{-2} of $j(H_2)$; see Figure 1b) is produced at the cathode and anode due to the crossover of H_2 and O_2 through the PEM. The increase in the water content at the anode/PEM interface in the presence of silica NPs can decrease the degradation rate of the Nafion PEM, considering the RH dependence of the degradation rate.[23,24] Furthermore, because the water molecule has been reported to stabilize H_2O_2 adsorbed on silica,[29] the increase in water content in the anode CL in the presence of silica NPs can promote formation of the silica–H_2O_2 complex, which can suppress the formation of radicals as discussed in the previous section. It has also been reported that silica or dissolved silicate adsorbed on the surface of Fe(III) oxide or hydroxide blocks the Fenton-like reaction (decomposition of H_2O_2 to form radicals) at room temperature.[32,33] This mechanism has not been confirmed yet for single cells operated at 90 °C, but it is worth examining, in the near future, considering the very mild decomposition of the Nafion PEM accompanying silica addition shown in Figure 1.

Next, we focus on why the effects of silica rather decreased at 0.4-SiO_2 regarding the durability of the PEM (increases in FER in the OCV test and $j(H_2O_2)$ in the m-CFDE measurements) and cell performance (increase in R_{ohm}, together with slight decreases in MA and $j_{@0.7V}$). The particle size of silica in the colloidal solution of the composition identical with the anode catalyst paste (without adding Pt/C catalyst powder alone) was measured as a function of the volume ratio of silica by the dynamic light scattering (DLS) technique. As shown in Figure S9, monodisperse silica NPs with sizes of 2.0, 2.8, and 11.5 nm were observed for the volume ratios of silica corresponding to V_{SiO_2}/V_C values of 0.1, 0.2, and 0.3, respectively. Such particle sizes were found to be maintained stably in the presence of Nafion binder (N/C = 0.7) in the colloidal solution, whereas silica particles without addition of Nafion agglomerated shortly (in a few hours). It has been reported that Nafion binder in a colloidal solution could adsorb on positively charged (H^+-adsorbed) oxide NPs, resulting in a stable nanoparticulate state.[34] In contrast, at the larger volume ratio of V_{SiO_2}/V_C = 0.4, the primary particle size increased to about 170 nm with an agglomerate peak of 770 nm even at N/C = 0.7. Therefore, it is considered that such an agglomeration of silica, which could lead to a nonuniform distribution, is the predominant reason for the decreased effects of silica at V_{SiO_2}/V_C = 0.4.

The durability of MEAs with the anode CL including silica will be tested under load cycle conditions[35,36] in the near future. Further research, including theoretical calculations, as well as in situ measurements are planned. The results will be presented elsewhere.

4. CONCLUSIONS

A remarkably prolonged (4 times) lifetime of the Nafion PEM, accompanied by an improved output performance in the steady-state *I*–*E* curves at low RH, have been demonstrated in a single cell by adding silica NPs to the Pt/C anode CL (V_{SiO_2}/V_C between 0.2 and 0.3) at 90 °C. The Si component was found to be uniformly dispersed in the anode CL and remain in the CL after a pressurized OCV test for periods as long as 600 h. It was clarified by hydrodynamic voltammograms in a half-cell (m-CFDE) at 90 °C that the addition of silica NPs resulted in the H_2O_2 formation rate at Pt/C decreasing remarkably. The silica NPs played an important role in increasing the water content in the MEA, which improved the *I*–*E* performance via enhanced Pt effectiveness as well as higher proton conductance to reduce *IR* loss. Such an increased water content, with certainty, also contributed to extend the lifetime of the Nafion PEM.

■ ASSOCIATED CONTENT

Supporting Information

The Supporting Information is available free of charge at https://pubs.acs.org/doi/10.1021/acsami.3c01392.

Compositions of anode CLs prepared (Table S1); dependence of lifetime of Nafion PEM on SiO_2 volume ratio in the AST (Figure S1); linear sweep voltammograms measured during the AST of single cells with various anode CLs (Figure S2); TEM images of anode CL with V_{SiO_2}/V_C = 0.2 in the pristine state (Figure S3); XRD of silica after drying the colloidal solution (Figure S4); H_2O_2 formation rates $j(H_2O_2)$ on Pt/C with various SiO_2 ratios measured by m-CFDE at 80 °C (Figure S5); dependence of $j(H_2O_2)$, kinetically controlled mass activities, and specific activities for the HOR at Pt/C on SiO_2 volume ratio at 80 °C (Figure S6); *I*–*E* curves and R_{ohm} of single cells operated at 40% RH//40% RH (Figure S7); 20% RH//60% RH (Figure S8), and particle size distribution of silica in the colloidal solution measured by DLS (Figure S9) (PDF)

■ AUTHOR INFORMATION

Corresponding Author

Hiroyuki Uchida − *Clean Energy Research Center, University of Yamanashi, Kofu 400-8510, Japan;* orcid.org/0000-0001-6718-5431; Email: h-uchida@yamanashi.ac.jp

Authors

Mohamed R. Berber − *Clean Energy Research Center, University of Yamanashi, Kofu 400-8510, Japan;* orcid.org/0000-0002-4468-0998

Muhammad Imran − *Clean Energy Research Center, University of Yamanashi, Kofu 400-8510, Japan;* orcid.org/0000-0001-5288-7166

Hanako Nishino − *Hydrogen Fuel Cell Nanomaterials Center, University of Yamanashi, Kofu 400-0021, Japan*

Complete contact information is available at: https://pubs.acs.org/10.1021/acsami.3c01392

Notes

The authors declare no competing financial interest.

■ ACKNOWLEDGMENTS

This work was supported by funds for the "R&D of novel anode catalyst project" in the "Collaborative industry-academia-government R&D project for solving common challenges toward dramatically expanded use of fuel cells" from the New Energy and Industrial Technology Development Organization (NEDO) of Japan. The authors thank Prof. Donald A. Tryk (Hydrogen and Fuel Cell Nanomaterials Center, University of Yamanashi) for his kind advice.

REFERENCES

(1) Banham, D.; Ye, S. Y. Current Status and Future Development of Catalyst Materials and Catalyst Layers for Proton Exchange Membrane Fuel Cells: An Industrial Perspective. *ACS Energy Lett.* **2017**, *2* (3), 629−638.

(2) Xie, M.; Chu, T.; Wang, T.; Wan, K.; Yang, D.; Li, B.; Ming, P.; Zhang, C. Preparation, Performance and Challenges of Catalyst Layer for Proton Exchange Membrane Fuel Cell. *Membranes (Basel)* **2021**, *11* (11), 879.

(3) Sun, Y.; Polani, S.; Luo, F.; Ott, S.; Strasser, P.; Dionigi, F. Advancements in Cathode Catalyst and Cathode Layer Design for Proton Exchange Membrane Fuel Cells. *Nat. Commun.* **2021**, *12* (1), 5984.

(4) Zatoń, M.; Rozière, J.; Jones, D. J. Current Understanding of Chemical Degradation Mechanisms of Perfluorosulfonic Acid Membranes and Their Mitigation Strategies: a Review. *Sustain. Energy Fuels* **2017**, *1* (3), 409−438.

(5) Li, T.; Shen, J.; Chen, G.; Guo, S.; Xie, G. Performance Comparison of Proton Exchange Membrane Fuel Cells with Nafion and Aquivion Perfluorosulfonic Acids with Different Equivalent Weights as the Electrode Binders. *ACS Omega* **2020**, *5* (28), 17628−17636.

(6) LaConti, A. B.; Hamdan, M.; McDonald, R. C. Mechanisms of Membrane Degradation. In *Handbook of Fuel Cells, Fundamentals−Technology and Applications*; Vielstich, W.; Lamm, A.; Gasteiger, H. A., Eds.; John Wiley & Sons: New York, 2003; Vol. 3, pp 647−662.

(7) Endoh, E. Development of Highly Durable PFSA Membrane and MEA for PEMFC Under High Temperature and Low Humidity Conditions. *ECS Trans.* **2008**, *16* (2), 1229−1240.

(8) Coms, F. D.; Liu, H.; Owejan, J. E. Mitigation of Perfluorosulfonic Acid Membrane Chemical Degradation Using Cerium and Manganese Ions. *ECS Trans.* **2008**, *16* (2), 1735−1747.

(9) Zhao, D.; Yi, B. L.; Zhang, H. M.; Yu, H. M. MnO_2/SiO_2-SO_3H Nanocomposite as Hydrogen Peroxide Scavenger for Durability Improvement in Proton Exchange Membranes. *J. Membr. Sci.* **2010**, *346* (1), 143−151.

(10) Zatoń, M.; Prélot, B.; Donzel, N.; Rozière, J.; Jones, D. J. Migration of Ce and Mn Ions in PEMFC and Its Impact on PFSA Membrane Degradation. *J. Electrochem. Soc.* **2018**, *165* (6), F3281−F3289.

(11) Thmaini, N.; Charradi, K.; Ahmed, Z.; Aranda, P.; Chtourou, R. Nafion/SiO_2@TiO_2-Palygorskite Membranes with Improved Proton Conductivity. *J. Appl. Polym. Sci.* **2022**, *139* (21), 52208.

(12) Baker, A. M.; Babu, S. K.; Mukundan, R.; Advani, S. G.; Prasad, A. K.; Spernjak, D.; Borup, R. L. Cerium Ion Mobility and Diffusivity Rates in Perfluorosulfonic Acid Membranes Measured via Hydrogen Pump Operation. *J. Electrochemi. Soc.* **2017**, *164* (12), F1272−F1278.

(13) Wong, K. H.; Kjeang, E. Simulation of Performance Tradeoffs in Ceria Supported Polymer Electrolyte Fuel Cells. *J. Electrochem. Soc.* **2019**, *166* (2), F128−F136.

(14) Watanabe, M.; Uchida, H.; Seki, Y.; Emori, M.; Stonehart, P. Self-Humidifying Polymer Electrolyte Membranes for Fuel Cells. *J. Electrochem. Soc.* **1996**, *143* (12), 3847−3852.

(15) Hagihara, H.; Uchida, H.; Watanabe, M. Preparation of Highly Dispersed SiO_2 and Pt Particles in Nafion® 112 for Self-humidifying Electrolyte Membranes in Fuel Cells. *Electrochim. Acta* **2006**, *51* (19), 3979−3985.

(16) Inoue, N.; Uchida, M.; Watanabe, M.; Uchida, H. SiO_2-Containing Catalyst Layers for PEFCs Operating under Low Humidity. *Electrochem. Commun.* **2012**, *16* (1), 100−102.

(17) Inoue, N.; Uchida, M.; Watanabe, M.; Uchida, H. Experimental Analyses of Low Humidity Operation Properties of SiO_2-Containing Catalyst Layers for Polymer Electrolyte Fuel Cells. *Electrochim. Acta* **2013**, *88*, 807−813.

(18) Park, K.; Goto, M.; So, M. G.; Takenaka, S.; Tsuge, Y.; Inoue, G. Influence of Cathode Catalyst Layer with SiO_2-Coated Pt/Ketjen Black Catalysts on Performance for Polymer Electrolyte Fuel Cells. *Catalysts* **2021**, *11* (12), 1517.

(19) Shimizu, R.; Tsuji, J.; Sato, N.; Takano, J.; Itami, S.; Kusakabe, M.; Miyatake, K.; Iiyama, A.; Uchida, M. Durability and Degradation Analysis of Hydrocarbon Ionomer Membranes in Polymer Electrolyte Fuel Cells Accelerated Stress Evaluation. *J. Power Sources* **2017**, *367*, 63−71.

(20) Kaur, H.; Chaudhary, S.; Kaur, H.; Chaudhary, M.; Jena, K. C. Hydrolysis and Condensation of Tetraethyl Orthosilicate at the Air−Aqueous Interface: Implications for Silica Nanoparticle Formation. *ACS Appl. Mater. Interfaces* **2022**, *5* (1), 411−422.

(21) Uchida, H.; Shi, G.; Imran, M.; Tryk, D. A. Particle-Size Effect of Pt Anode Catalysts on H_2O_2 Production Rate and H_2 Oxidation Activity at 20 to 80 °C. *J. Electrochem. Soc.* **2022**, *169* (1), 014516.

(22) U.S. DRIVE Fuel Cell Tech. Team Road Map (November 2017), pp 21. https://www.energy.gov/sites/default/files/2017/11/f46/FCTT_Roadmap_Nov_2017_FINAL.pdf.

(23) Sethuraman, V. A.; Weidner, J. W.; Haug, A. T.; Protsailo, L. V. Durability of Perfluorosulfonic Acid and Hydrocarbon Membranes: Effect of Humidity and Temperature. *J. Electrochem. Soc.* **2008**, *155* (2), B119−B124.

(24) Rodgers, M. P.; Bonville, L. J.; Mukundan, R.; Borup, R. L.; Ahluwalia, R.; Beattie, P.; Brooker, R. P.; Mohajeri, N.; Kunz, H. R.; Slattery, D. K.; Fenton, J. M. Perfluorinated Sulfonic Acid Membrane and Membrane Electrode Assembly Degradation Correlating Accelerated Stress Testing and Lifetime Testing. *ECS Trans.* **2013**, *58* (1), 129−148.

(25) Shi, G.; Tryk, D. A.; Iwataki, T.; Yano, H.; Uchida, M.; Iiyama, A.; Uchida, H. Unparalleled Mitigation of Membrane Degradation in Fuel Cells via a Counter-Intuitive Approach: Suppression of H_2O_2 Production at the Hydrogen Anode using a Pt skin−PtCo Catalyst. *J. Mater. Chem. A* **2020**, *8* (3), 1091−1094.

(26) Uchida, H.; Ikeda, N.; Watanabe, M. Electrochemical Quartz Crystal Microbalance Study of Copper Adatoms on Gold Electrodes Part II. Further Discussion on the Specific Adsorption of Anions from Solutions of Perchloric and Sulfuric Acid. *J. Electroanal. Chem.* **1997**, *424* (1−2), 5−12.

(27) Mauritz, K. A.; Moore, R. B. State of Understanfing Nafion. *Chem. Rev.* **2004**, *104*, 4535−4585.

(28) Shi, G. Y.; Yano, H.; Tryk, D. A.; Matsumoto, M.; Tanida, H.; Arao, M.; Imai, H.; Inukai, J.; Iiyama, A.; Uchida, H. Weakened CO Adsorption and Enhanced Structural Integrity of a Stabilized Pt skin/PtCo Hydrogen Oxidation Catalyst Analysed by In situ X-ray Absorption Spectroscopy. *Catal. Sci. Technol.* **2017**, *7* (4), 6124−6131.

(29) Żegliński, J.; Piotrowski, G. P.; Piękoś, R. A Study of Interaction Between Hydrogen Peroxide and Silica Gel by FTIR Spectroscopy and Quantum Chemistry. *J. Mol. Struct.* **2006**, *794* (1−3), 83−91.

(30) Lee, M.; Uchida, M.; Yano, H.; Tryk, D. A.; Uchida, H.; Watanabe, M. New Evaluation Method for the Effectiveness of Platinum/carbon Electrocatalysts under Operating Conditions. *Electrochim. Acta* **2010**, *55* (28), 8504−8512.

(31) Yoda, T.; Shimura, T.; Bae, B.; Miyatake, K.; Uchida, M.; Uchida, H.; Watanabe, M. Gas Diffusion Electrodes Containing Sulfonated Poly (arylene ether) Ionomer for PEFCs Part 1. Effect of Humidity on the Cathode Performance. *Electrochim. Acta* **2009**, *54* (18), 4328−4333.

(32) Pham, A. L.; Doyle, F. M.; Sedlak, D. L. Inhibitory Effect of Dissolved Silica on H_2O_2 Decomposition by Iron(III) and Manganese(IV) Oxides: Implications for H_2O_2-based In situ Chemical Oxidation. *Environ. Sci. Technol.* **2012**, *46* (2), 1055−62.

(33) Hanna, K. Comment on "Inhibitory Effect of Dissolved Silica on H_2O_2 Decomposition by Iron(III) and Manganese(IV) Oxides: Implications for H_2O_2-based In situ Chemical Oxidation". *Environ. Sci. Technol.* **2012**, *46* (6), 3591−2.

(34) Miyoshi, H.; Tanaka, K.; Uchida, H.; Yoneyama, H.; Mori, H.; Sakata, T. Photoelectrochemical Properties of Fe_2O_3 Microcrystallites Prepared in Nafion. *J. Electroanal. Chem.* **1990**, *295* (1), 71−78.

(35) Takei, C.; Kakinuma, K.; Kawashima, K.; Tashiro, K.; Watanabe, M.; Uchida, M. Load Cycle Durability of a Graphitized

https://doi.org/10.1021/acsami.3c01392
ACS Appl. Mater. Interfaces 2023, 15, 13219−13227

Carbon Black-Supported Platinum Catalyst in Polymer Electrolyte Fuel Cell Cathodes. *J. Power Sources* **2016**, *324*, 729−737.
(36) Yuan, H.; Dai, H.; Ming, P.; Zhao, L.; Tang, W.; Wei, X. Understanding Dynamic Behavior of Proton Exchange Membrane Fuel Cell in the View of Internal Dynamics Based on Impedance. *Chem. Eng. J.* **2022**, *431*, 134035.

https://doi.org/10.1021/acsami.3c01392
ACS Appl. Mater. Interfaces 2023, 15, 13219−13227